Reassessment of the Antarctic surface mass balance using calibrated output of a regional atmospheric climate model

W. J. van de Berg,[1] M. R. van den Broeke,[1] C. H. Reijmer,[1] and E. van Meijgaard[2]

Received 13 July 2005; revised 5 December 2005; accepted 13 February 2006; published 3 June 2006.

[1] A detailed comparison of model-simulated and observed Antarctic surface mass balance (SMB) is presented, using output of a regional atmospheric climate model (RACMO2/ANT) for the period 1980 to 2004. All available SMB observations from Antarctica (N = 1900) are used for the comparison, except clearly erroneous observations and data which are in areas where dominant SMB patterns occur on scales smaller than the model resolution. A high correlation is found (r = 0.82), while the regression slope (1.2) indicates that the model slightly overemphasizes SMB gradients. Comparing the model SMB with the latest SMB compilation, a similarly high correlation is found (r = 0.79), but the regression slope is much too steep because model-simulated SMB agrees less with the compilation in data-sparse regions. Model-simulated SMB resembles the observed SMB as a function of elevation very well. This is used to calibrate model-simulated SMB to reassess the contemporary Antarctic SMB. Compared to the latest SMB compilation, calibrated model-simulated SMB is up to 1 m yr^{-1} higher in the coastal zones of East and West Antarctica, which are without exception in areas with few observations. As a result, the SMB integrated over the grounded ice sheet (171 ± 3 mm yr^{-1}) exceeds previous estimates by as much as 15%. Support or falsification of this model result can only be found in new SMB observations from high accumulation regions.

Citation: van de Berg, W. J., M. R. van den Broeke, C. H. Reijmer, and E. van Meijgaard (2006), Reassessment of the Antarctic surface mass balance using calibrated output of a regional atmospheric climate model, *J. Geophys. Res.*, *111*, D11104, doi:10.1029/2005JD006495.

1. Introduction

[2] An important aspect of the influence of Antarctica on the global climate system is the storage of fresh water in ice, which lowers sea level by about 61 m [*Huybrechts et al.*, 2000]. Changes in the ice volume on Antarctica, i.e., a nonzero mass balance of the grounded ice sheet (GIS), directly changes global sea level. Several Antarctic ice drainage basins have been reported to be out of balance. In coastal West Antarctica, the Pine Island and Thwaites glaciers discharge each year about 250 km^3 of ice into the ocean, 60% more than is estimated to accumulate within their catchment basins [*Thomas et al.*, 2004]. This is sufficient for a global sea level rise of 0.24 mm yr^{-1}, a very significant number compared to the value of -0.1 ± 0.1 mm yr^{-1} that was estimated for the contribution of the whole Antarctic ice sheet in the last century [*Intergovernmental Panel on Climate Change (IPCC)*, 2001]. In contrast to the retreat in West Antarctica, satellite radar altimetry suggests that the ice sheet thickened between 1992 and 2003 in East Antarctica, lowering sea level by 0.12 mm yr^{-1} [*Davis et al.*, 2005].

[3] During the last decade, solid ice fluxes are determined with much higher precision because surface elevation changes and surface velocities can be measured by satellites [cf. *Thomas et al.*, 2004]. However, such a step forward has not been made for the surface mass balance (SMB), because it cannot directly be measured by satellites. Recent SMB compilations are based on observations first of all, but in situ observations are lacking for vast areas of Antarctica. *Giovinetto and Zwally* [2000] visually interpolated the observations, and *Vaughan et al.* [1999] (hereinafter referred to as V99) used passive microwave data from satellites for their interpolation. Atmospheric models provide another estimate of the Antarctic SMB [*Bromwich et al.*, 2004; *Genthon and Krinner*, 2001]. Model results are usually validated by subtracting the SMB compilation of V99 from the model-simulated SMB and visually interpreting the differences. In that way model results can only be qualitatively assessed. A similar statement can be made about simulation of the Greenland SMB [*Dethloff et al.*, 2002; *Box et al.*, 2004, 2006], where ablation plays a major role.

[4] Here we carry out a more detailed and quantitative evaluation of model-simulated Antarctic SMB. The simulated SMB includes solid precipitation, sublimation and snowmelt. After the evaluation, we slightly calibrate model

[1] Institute for Marine and Atmospheric Research Utrecht, University of Utrecht, Utrecht, Netherlands.
[2] Royal Dutch Meteorological Institute (KNMI), De Bilt, Netherlands.

0148-0227/06/2005JD006495$09.00

SMB to match observations, in order to get a best possible estimate of the contemporary Antarctic SMB. This reassessed SMB primarily provides a new estimate of the SMB where few observations are available.

[5] We present a description of the model in section 2. In section 3, SMB observations are presented and we describe how model values are interpolated to the location of the observations, and how observationally dense areas are treated. In section 4, we statistically compare model results with the compilation of V99 and with the derived observational data set. We consider the importance of temporal variability compared to spatial variability. The section is concluded with a verification of model-simulated SMB as a function of elevation for East and West Antarctica separately. Section 5 discusses the statistical robustness of results. Finally, model-simulated and observed SMB are combined to derive a best estimate of contemporary Antarctic SMB. Conclusions are drawn in section 6.

2. Model Description

[6] RACMO2/ANT is adapted from the second version of the Regional Atmospheric Climate Model (RACMO2). The atmospheric dynamics description of RACMO2 originates from the High-Resolution Limited Area Model (HIRLAM), version 5.0.6 [*Undén et al.*, 2002]. The physical processes are adopted from the European Centre for Medium-Range Weather Forecasts (ECMWF), cycle CY23R4 [*White*, 2001].

[7] The horizontal resolution of RACMO2/ANT is ~55 km. The model has 40 hybrid levels in the vertical, of which the lowest is ~10 m above the surface. Hybrid levels follow the topography close to the surface and pressure levels at higher altitudes. ECMWF Reanalysis (ERA-40) fields force the model at the lateral boundaries, while the interior of the domain is allowed to evolve freely. ECMWF operational analyses have been used to extend the model time series by 28 months until the end of 2004. Although the operational cycle is processed at double horizontal resolution compared to ERA-40, both products have been derived with a very similar formulation of the same numerical weather model and we consider the extension a useful and almost consistent continuation. Ice free sea surface temperature and the sea ice fraction are prescribed from ERA-40. Sea ice has a thickness of 1 m.

[8] Several physical parameterizations within RACMO2/ANT have been changed to better represent Antarctic conditions. The snow albedo parameterization of *Van den Hurk and Viterbo* [2003] was implemented. For freezing conditions, the albedo decay in this parameterization is diminished proportional with the forth power of the temperature. As a result, the albedo of snow remains almost constant below −10°C. Furthermore, the surface roughness length for momentum was reduced [*Reijmer et al.*, 2004b], and the expression presented by *Andreas* [1987] was applied to calculate the surface roughness lengths of heat and moisture over snow surfaces. A four layer snow model was added to improve subsurface heat fluxes into the snowpack. These adjustments and their positive effect on the boundary layer, together with the setup of RACMO2/ANT, are described by *Reijmer et al.* [2004a].

[9] In addition, horizontal diffusion of moisture has been decreased, which reduces artificial uphill moisture transport [*Lenderink et al.*, 2003]. Concentrations of CO_2 and other trace gasses were varied following IPCC 2001.

[10] Finally, a correction was applied to the precipitation scheme. The original scheme puts the generated rain to snow ratio equal to the cloud water to cloud ice ratio. The ratio is a parabolic function of temperature and favors cloud ice for temperatures below −7°C. Although such a cloud ice fraction closely below 0°C is unrealistically high, it still overestimates the rain fraction of supercooled clouds. Supercooled clouds can only generate rain if the cloud contains cloud water only, which rarely happens. Snow formation processes dominate in the prevailing mixed clouds [*Rogers and Yau*, 1989]. This model flaw is corrected by imposing that clouds below −1°C form snow only. The effect of the additional energy release in the cloud on the temperature profile was found to be small.

[11] *Bromwich and Fogt* [2004] and *Sterl* [2004] have shown that the quality of ERA-40 before 1980 is poor for the Southern Hemisphere. The incorporation of satellite data in 1979 causes a sudden increase of model-simulated SMB for ERA-40 as well as for RACMO2/ANT [*Van de Berg et al.*, 2006]. Therefore we only use model results for the period 1980 to 2004.

3. Observations and Data Handling

[12] Figure 1 shows the observed values of SMB that are used for the comparison. This data set is a revised version of that used by V99, which comprised 1796 observations. Furthermore, 236 new observations described by *Van den Broeke et al.* [1999], *Frezzotti et al.* [2004], *Kärlof et al.* [2000], *Kaspari et al.* [2004], *Magand et al.* [2004], *Oerter et al.* [1999, 2000], and *Smith et al.* [2002] have been added. For the Antarctic Peninsula, data presented by *Turner et al.* [2002] have been used. The observations within the data set have been derived with various measurement techniques, for example stake arrays, bomb horizons or chemical analysis of ice cores. As a result, the time period covered by an observation varies from only a few years to more than a century. Single-year observations have been discarded.

[13] Observations were checked for processing errors by comparing the stated elevation with Radarsat Antarctic Mapping Project (RAMP) elevations [*Liu et al.*, 2001], because an unreasonable elevation often indicates an error in the geographical location. Such possible errors and missing information on elevation and time horizons of the accumulation observations have been looked up in the original publications as much as possible. For binning purposes (see section 4.4), RAMP elevations have been used for unrecoverable elevations.

[14] In the next paragraphs the arguments for omitting three areas are given, followed by the method of how observed SMB is compared with model-simulated SMB. Lastly, a description is given of the treatment of areas with dense observations. The influence of data processing on the results will be discussed in section 5.1.

3.1. Excluded Areas

[15] Observations from three areas are excluded from the comparison between model-simulated and observed SMB, namely, coastal Marie Byrd Land (MBL), the Antarctic

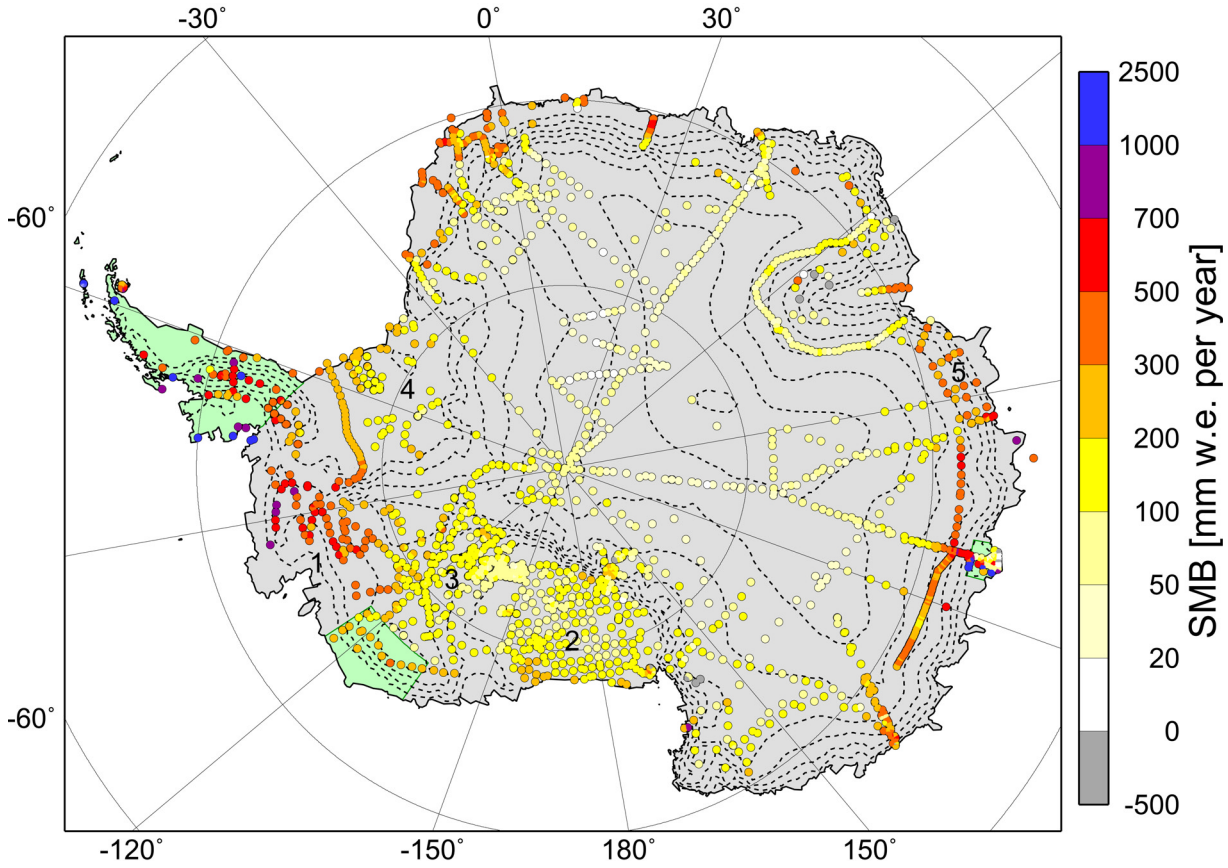

Figure 1. Observed surface mass balance (SMB) over Antarctica. Circles mark measurements. In case of clustered observations a continuous map is drawn. The excluded areas are marked with a green background. The numbers mark regions in Antarctica: 1, Pine Island and Thwaites Glacier; 2, Ross Ice Shelf; 3, Siple Coast; 4, Flichnerr Ronne Ice Shelf; 5, Wilhelm II Land.

Peninsula and Law Dome, indicated by green areas in Figure 1.

[16] The observations of *Pirrit and Doumani* [1961], made during the Marie Byrd Land traverse in the austral summer of 1959–1960, are the only available observations from coastal MBL. They estimated the SMB using snow density, descriptive stratigraphy, pit wall photographs and rammsonde hardness. The snow density was determined up to a depth of 10 m, while the pits were 3 m deep (∼1 m w.e.). Using this information, they found SMB rates between 180 and 320 mm w.e. yr^{-1}. Although visual interpretation has been shown to work well for plateau sites, it is not very reliable in areas of high accumulation, nor is it fully independent of the observer's expectation [cf. *Bull*, 1971]. A snow pit should cover at least one annual layer, so a snow pit depth of 3 m indicates that a larger annual accumulation rate was not expected. Passive microwave data, as presented by *Zwally and Giovinetto* [1995], do suggest a larger accumulation rate for this region. We decided to exclude all observations of *Pirrit and Doumani* [1961] north of 77° South and between 115° and 135° West. The remaining data set still contains observations that are based on visual interpretation techniques, but we chose to exclude only observations that are clearly erroneous.

[17] We also exclude two regions with a combination of relatively high observational density and strong SMB gradients due to small-scale topography. The first area is Law Dome, where the typical length scale of elevation and accumulation variability is about 10 km. Exclusion is reasonable because the model surface topography of this region is smoothed, since the model resolution is ∼55 km. Nevertheless, a similarity between observed (Figure 2b) [*van Ommen et al.*, 2004] and model-simulated SMB (Figure 2a) is clearly present. The strong east-west SMB gradient as well as the magnitudes of maximum and minimum SMB compare well with *van Ommen et al.* [2004]. The lower model resolution mainly shifts and smoothes the pattern. Surprisingly, the SMB observations in our observational data set, represented by the circles in Figure 2a, are not consistent with the pattern of *van Ommen et al.* [2004]. Although the area of Law Dome is relatively small, these observations could seriously bias the regression due to its large SMB gradients.

[18] The Antarctic Peninsula is the second area where topography is dominated by small-scale features. As a result, SMB observations are often not representative for an area that approaches the model grid box size and model topography does not always capture the characteristic topographic features. A second reason for leaving out the Antarctic Peninsula is the SMB behavior with elevation. On the Antarctic mainland, accumulation rates are rather low and decrease with height. On the Antarctic Peninsula,

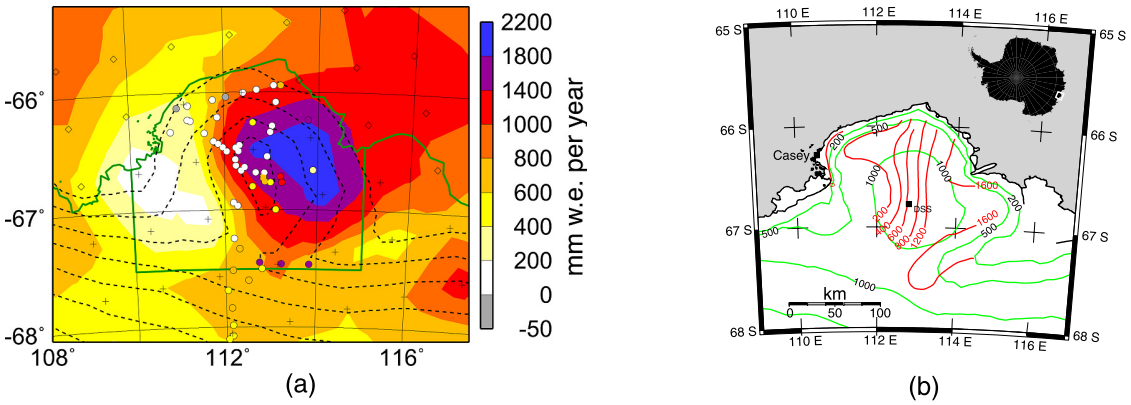

Figure 2. (a) Model-simulated and observed SMB over Law Dome. Observations are indicated by circles. Crosses mark land grid points, and diamonds mark grid points on sea, for which the annual solid precipitation is displayed. The dashed contours display the model surface elevation with an interval of 250 m. The green borders indicate the edges of the land and ice shelves and also the border of the excluded area. (b) Pattern based on SMB observations from [*van Ommen et al.*, 2004] (reprinted with permission from the International Glaciological Society), which disagrees with the observations in Figure 2a.

the magnitude of the SMB can be one order of magnitude larger and the SMB increases with height. Hence we exclude the Antarctic Peninsula in our comparison.

[19] Nevertheless, the model-simulated SMB for the Antarctic Peninsula (Figure 3) is briefly evaluated here. Although the limited model resolution smoothes the topography, the model-simulated SMB patterns are reasonable. For example, accumulation patterns in King George VI Sound are modeled well, because the model topography captures the sheltered position of the sound. The SMB on Dyer Plateau is overestimated, probably because the topographic shape of the Dyer Plateau in the model is still a ridge instead of a plateau. Smaller grid spacing indeed improves model-simulated SMB patterns, as shown by *Van Lipzig et al.* [2004]. They also showed that the influence of snow drift on the plateau of the Antarctic Peninsula cannot be neglected, however, this process is not included in RACMO2/ANT.

[20] The model-simulated SMB behaves rather linearly with elevation in the northern part of the peninsula (Figure 4), in agreement with the linear relationship that was found by *Turner et al.* [2002] based on SMB observations. The model-simulated SMB increases 3.3 mm w.e. yr^{-1} per m elevation. This is much more than the 1.40 that was found by *Turner et al.* [2002] for the Western side of the peninsula. This might be due to the effects of snow drift which is not incorporated in RACMO2/ANT.

[21] A linear relation between elevation and SMB is less distinct for Alexander Island. If all grid points in Alexander Island are used, the SMB increases with 2.5 mm w.e. yr^{-1} per m elevation. The three large values (>2 m) in the north eastern corner of Alexander Island largely determine the slope. If these are omitted, the slope decreases to 1.2 mm w.e. yr^{-1} per m elevation. Figure 3 shows that the southern part of Alexander Island lies in the precipitation shadow of the northern hills. The relation between elevation and SMB is thus not equal above Alexander Island and in general lower than for the northern spine. These results differ from *Turner et al.* [2002], who uses the relationship of the

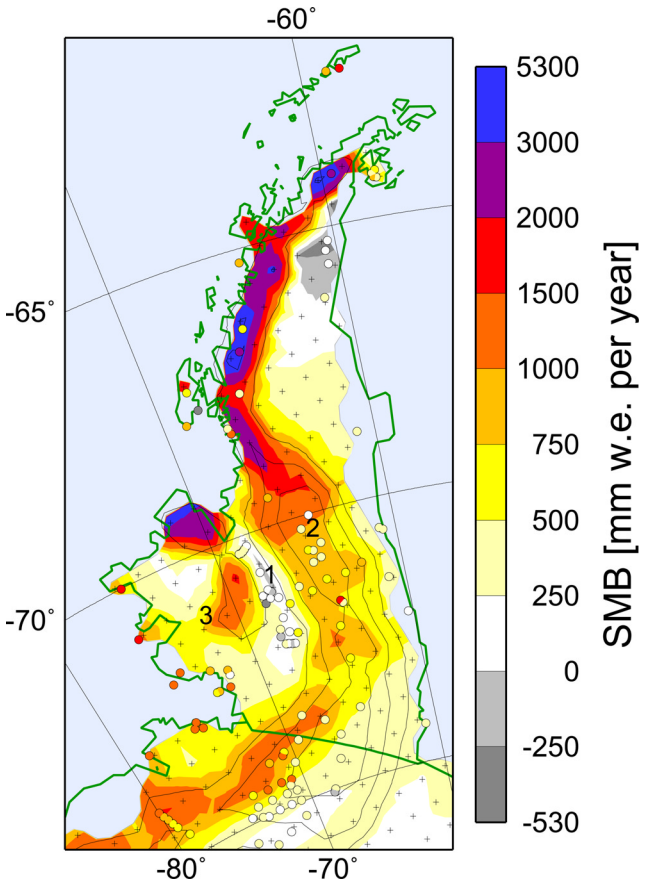

Figure 3. Model-simulated and observed SMB in the Antarctic Peninsula. Observations are indicated by circles. A light blue is used for model sea grid points. The crosses mark land grid points. Model elevation is drawn in thin black lines with 500 m interval. The thick green line indicates the actual edges of land and ice shelves and also the southern border of the peninsula. The numbers mark locations in the peninsula: 1, King George VI Sound; 2, Dyer Plateau; 3, Alexander Island.

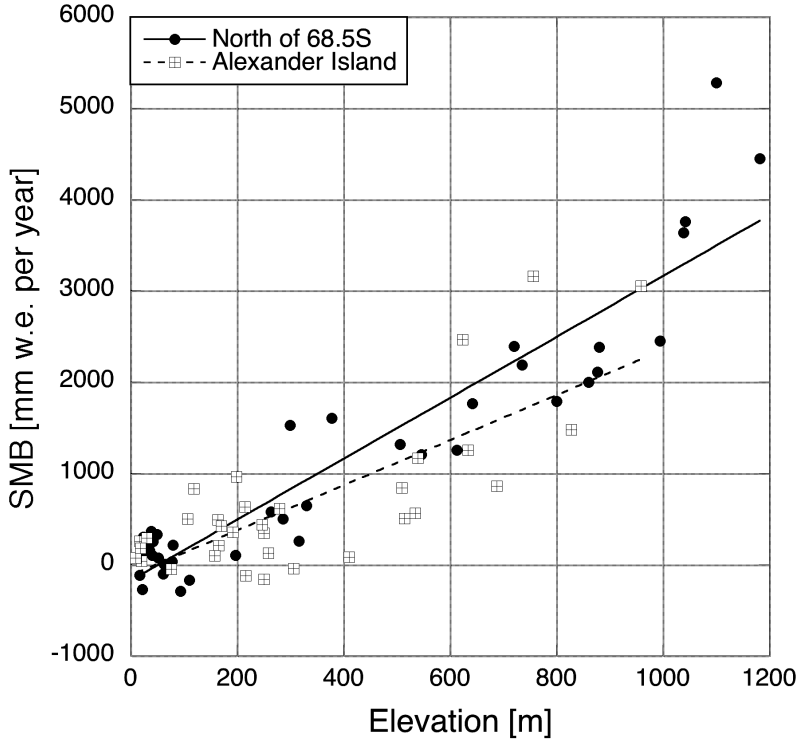

Figure 4. Relation between elevation and model-simulated SMB on the Antarctic Peninsula. The SMB of grid points north of 68.5°S (north of Dyer Plateau) and on Alexander Island are selected. The lines are linear fits.

northern peninsula to determine the SMB for Alexander Island as well.

[22] We may conclude that the model qualitatively resembles the SMB and its gradients in the complex regions of Law Dome and the Antarctic Peninsula, but that model resolution is not sufficient to enable a quantitative comparison.

3.2. Model Interpolation

[23] The remaining observations and model values are compared by interpolating model-simulated SMB to the location of the observation ($SMB_{g\rightarrow o}$). The interpolation is carried out using a weighted average of SMB of nearby model grid points. The weight $w_{g,o}$ of the model grid point g at the observation location o is given by

$$w_{g,o} = \alpha_o \cdot \max\left[0, 1 - \frac{dx_{g,o}}{dx_{\max}}\right] \tag{1}$$

in which $dx_{g,o}$ denotes the distance between the grid point and the observation location and $dx_{\max}$ the maximum distance for which a grid point affects the SMB of this location. The scaling factor α_o makes the sum of $w_{g,o}$ over all grid points one.

[24] The maximum distance $dx_{\max}$ is set to 55 km, equal to the grid distance. In that case the method boils down to a linear interpolation between the 4 surrounding grid points. For smaller $dx_{\max}$, $SMB_{g\rightarrow o}$ approaches the SMB of the most nearby grid point and for larger $dx_{\max}$ the model-simulated SMB field is smoothed. Observations that are outside the land domain of RACMO2/ANT are omitted.

3.3. Observationally Dense Areas

[25] If all SMB observations are equally distributed over Antarctica, all model grid points over the ice sheet would have the same weight when observations are compared with interpolated model values. In practice, observations are very irregularly distributed and are in some parts strongly clustered. If all observations would be given equal weights, areas in Antarctica with dense observations would be overrepresented in the comparison. Therefore weighting of observations is necessary. Nevertheless, the reliability of a regional value increases when the number of observation increases. An area with dense observations is given a somewhat greater weight than areas with sparse observations.

[26] The weighting starts with calculating the observation density d_g around grid point g as the sum of $w_{g,o}$ over all observations. Next, the observation density d_o around observation o is derived by

$$d_o = \sum_g \max\left[d_g, 1\right] \cdot w_{g,o} \tag{2}$$

in which a d_g less than one is set to one because a correction is only needed if the observation density exceeds 1. This d_o is scaled with a factor γ to get the weight β_o of an observation:

$$\beta_o = d_o^{\gamma} \tag{3}$$

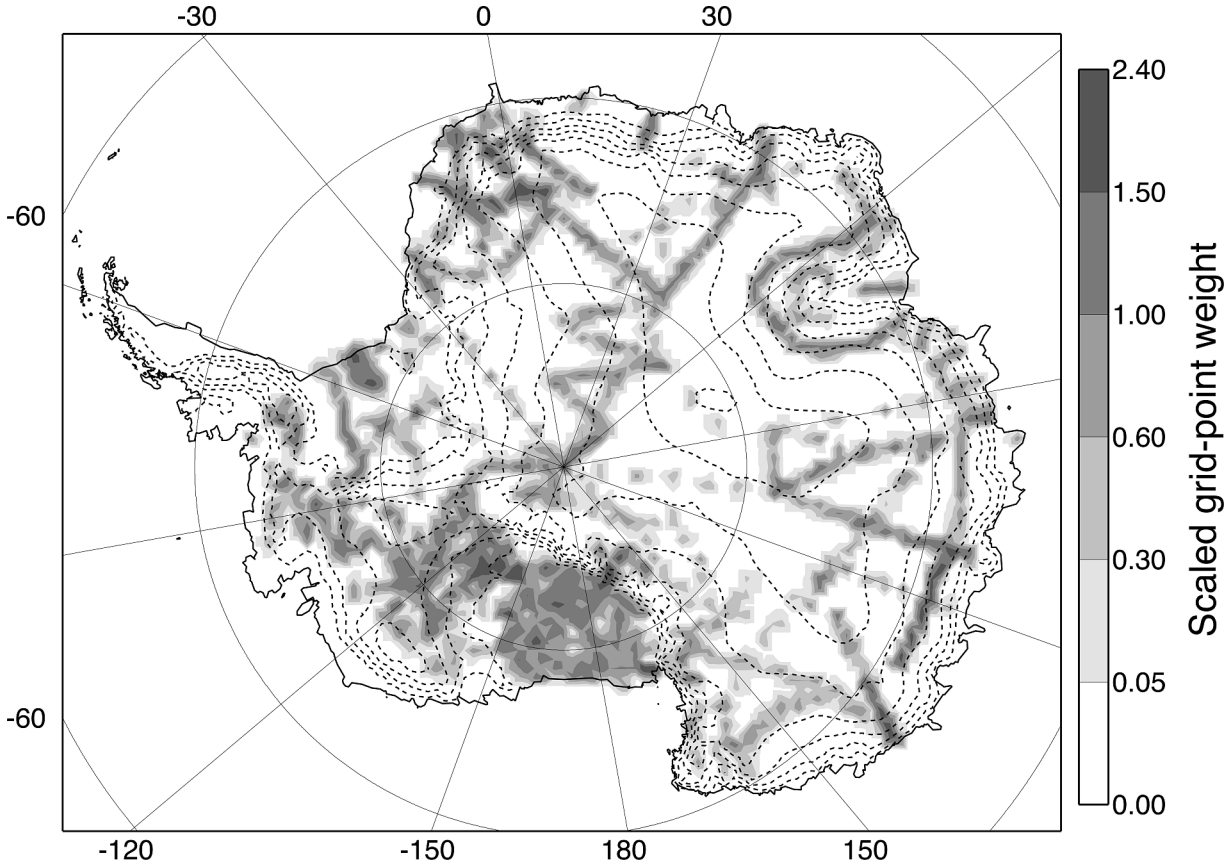

Figure 5. Scaled grid point weight (W_g) in Antarctica. Excluded areas have zero weight (see text).

and the scaled grid point weight W_g of a grid point is derived using

$$W_g = \sum_o \beta_o w_{g,o} \ . \tag{4}$$

[27] This scaled grid point weight W_g represents the weight of a grid point when weighted observations are compared with interpolated model-simulated values. The scaling factor γ is set to -0.75, to some extent an arbitrary value. For this value of γ, an area with uniform observation density $d_g = 16$ per grid point receives a double weight W_g compared to areas where $d_g = 1$. However, in practice observations are not uniformly distributed and there are only a few distinct locations with dense observations. The derivation of d_o incorporates some smoothing; therefore a grid point with a d_g less than 16 could still have a weight W_g that exceeds 2 if it is surrounded by grid points with low d_g.

[28] Figure 5 shows W_g as derived for the observations presented in Figure 1. Some parts of West Antarctica, like the Ross Ice Shelf and Siple Coast, are well covered by observations. The Filchner-Ronne Ice shelf, on the other hand, has a poor coverage. In East Antarctica, the coverage is on average so low that individual traverses can still be identified. The Antarctic Peninsula, coastal Marie Byrd Land and Law Dome have a zero weight because these areas are not included in the analysis.

[29] Finally, the weight β_o is used to determine an approximation of the observed SMB_o on the grid points ($SMB_{o\rightarrow g}$), using the formula

$$SMB_{o\rightarrow g} = \frac{\sum_o \beta_o w_{g,o} SMB_o}{\sum_o \beta_o w_{g,o}}. \tag{5}$$

4. Results

4.1. RACMO2/ANT Compared to V99

[30] Figure 6a depicts the difference between model simulated SMB and the compilation of V99. A clear general pattern is visible. The model-simulated SMB in the high interior of East Antarctica is generally 20 to 40 mm lower, being only 25 to 75% of V99. In contrast, the model-simulated SMB exceeds the compilation in general by 100 to 400 mm over the coastal slopes, except in the escarpment zone of Marie Byrd Land, where differences up to 1 m yr^{-1} are found. Furthermore, the model-simulated SMB compares favorable with V99 on the Ross Ice Shelf, the Filchner-Ronne Ice Shelf and the interior of West Antarctica. The model-simulated SMB in the Antarctic Peninsula shows a stronger elevation dependency than the compilation does.

[31] Figure 6b shows a scatterplot of model-simulated and compiled SMB with each point representing a grid

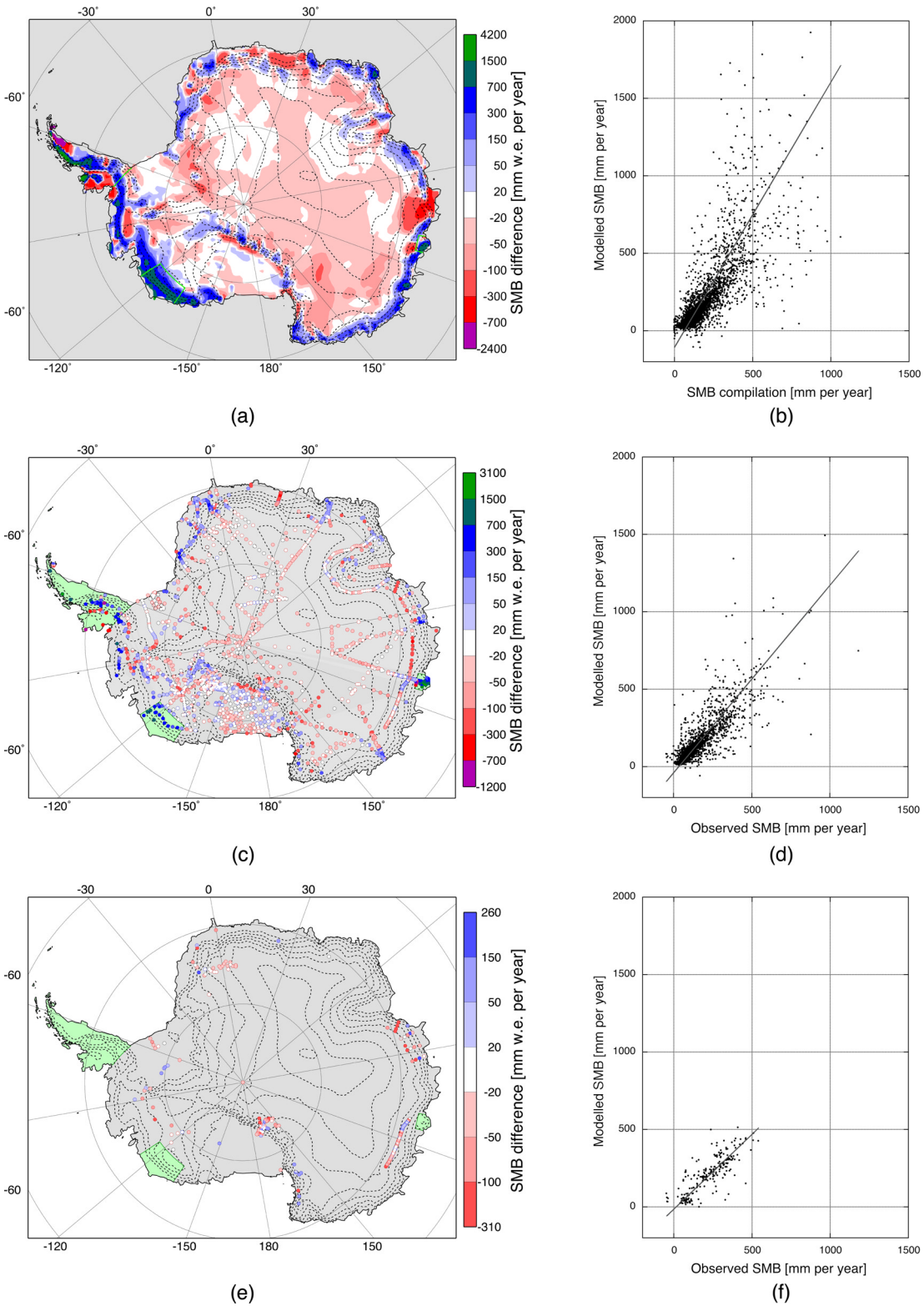

Figure 6. Comparison of model-simulated SMB with compiled and observed SMB. (a and b) Model results compared with V99. (c and d) Model results compared with observations. (e and f) Model results compared to observations, matching the time horizon of the observation. The excluded areas are bounded in Figure 6a by a solid green line. In Figures 6c and 6e these areas are drawn green. Figures 6a, 6c, and 6e show differences in mm yr^{-1}. Positive values are used if the model-simulated SMB is larger than the compiled/observed SMB. In Figure 6b a dot denotes a grid point; in Figures 6d and 6f a dot is an observation. The lines in Figures 6b, 6d, and 6f are regression lines. Fit properties are listed in Table 1, second, fourth, and sixth rows.

Table 1. Summary of SMB Results[a]

Model-Simulated SMB Compared to	N_{eff} ($\sum_o \beta_o$)	Correlation	Regression Slope	Mean SMB	
				V99/obs.	Model
V99, whole Antarctica	4534	0.70 ± 0.02	2.1 ± 0.12	169	184
V99, selected areas	4333	0.79 ± 0.011	1.71 ± 0.06	152	153
Observations, whole Antarctica	1281	0.69 ± 0.04	1.7 ± 0.2	171	182
Observations, selected areas	1225	0.82 ± 0.016	1.21 ± 0.06	157	149
Observations, within 1980–2004	136	0.81 ± 0.04	1.00 ± 0.10	204	192
Observations, within 1980–2004 + match time period	136	0.79 ± 0.05	0.96 ± 0.10	194	183

[a]The total weight of the data set (N_{eff}) is the sum of the individual observations weights β_o. The dimension of the mean SMB is mm w.e. yr^{-1}.

point of RACMO2/ANT. The fit is derived by minimizing the squared distances perpendicular to the fit line. Data from Law Dome, coastal Marie Byrd Land, and the Antarctic Peninsula are not included. The solid line is derived weighting all points equally. The correlation is 0.79 ± 0.011 and the slope of the best fit is 1.71 ± 0.06 (Table 1). Statistical error margins are derived by repeated fitting using a randomly chosen one third of the data set. The large regression slope links to the spatial pattern of a too dry simulated interior and an much wetter coastal zone. The mean SMB of RACMO2/ANT and V99 are also listed in Table 1. The mean values are nearly equal, which implies that in the model the drier plateau of East Antarctica is balanced by a wetter escarpment.

4.2. RACMO2/ANT Compared to Observations

[32] The differences between observed and model-simulated SMB at the observation locations are shown in Figure 6c. The qualitative similarity between Figures 6c and 6a is strong, unsurprisingly perhaps, because the majority of the observations shown here were used to construct the SMB compilation. However, new observations do not always confirm the compiled SMB in V99. The most distinct examples are the recent accumulation observations in Wilhelm II Land, which are more than twice the value in V99 [*Smith et al.*, 2002]. For comparison, RACMO2/ANT is on average 25% drier than these new observations.

[33] The negative SMB bias in the model data in the interior of East Antarctica is confirmed by Figure 6c. Averaged over elevation, the model-simulated SMB linearly decreases from 75% at 2500 m to only 30% of the observed SMB at 4000 m. The SMB on the large ice shelves agrees well and an overestimated accumulation along the coast is no longer that clear apparent in Figure 6c: areas with overestimated accumulation alternate with areas where accumulation is underestimated and the absolute values are much smaller than in Figure 6a. In line with this, the slope of the regression line, shown in Figure 6d, is 1.21 ± 0.06, which indicates that the distribution of SMB is well simulated. Furthermore, the correlation coefficient is 0.82 ± 0.016. Note that this correlation coefficient cannot be compared directly to the correlation derived in section 4.1, because the data amount has decreased and the spatial distribution has become less homogeneous. Although weighting of observations was applied, areas without any observations do not count in this comparison. All in all, RACMO2/ANT reliably reproduces the Antarctic SMB, although with slightly too strong SMB gradients from the interior to the coast.

4.3. Impact of Temporal Mismatch

[34] The results discussed in the previous section ignore temporal SMB variability. The model-simulated SMB is averaged over the period 1980 to 2004, while observations are also averages, but averaged over different time periods. This might be problematic, because the model-simulated SMB varies in time [*Van de Berg et al.*, 2006] and accumulation records may also show trends [e.g., *Hofstede et al.*, 2004]. Therefore ignoring temporal variability could decrease the correlation between observed and model-simulated SMB.

[35] In order to investigate the impact of temporal variability, observations are selected of which the time domain is covered at least for 80% by the model integration period (1980 to 2004). In many cases, however, the time span covered by an observation could not be recovered. Hence application of this criterion strongly reduces the number of observations. Yet most zones are still represented, except the highest part of the plateau of East Antarctica (Figure 6e and Table 1, fifth and sixth rows).

[36] The correlation of these observations to the mean model SMB is 0.81 ± 0.04. If the observations are compared with model SMB for the exact time period covered by the measurement, the correlation decreases slightly to 0.79 ± 0.05. Furthermore, the regression slope, which was close to one, does not vary significantly either. These minor changes confirm that temporal variability may be ignored when spatial variability is considered on timescales shorter than a century.

4.4. Elevation and SMB

[37] Elevation is one of the most important factors for the SMB. Furthermore, the topography of East and West Antarctica differs significantly. East Antarctica has a steep escarpment and coastal zone with less ice shelves, and a high and large plateau. West Antarctica includes the extensive Ross and Filchner-Ronne Ice Shelves, and the slopes are on average more gentle. Moreover, West Antarctica does not have a similarly distinct plateau as East Antarctica. Therefore we consider SMB as a function of elevation separately for East and West Antarctica, excluding the Antarctic Peninsula.

[38] Figures 7a and 7b compare model-simulated and observed SMB in 500 m elevation bins, for which the elevation of the SMB observation is used. The lowest bin

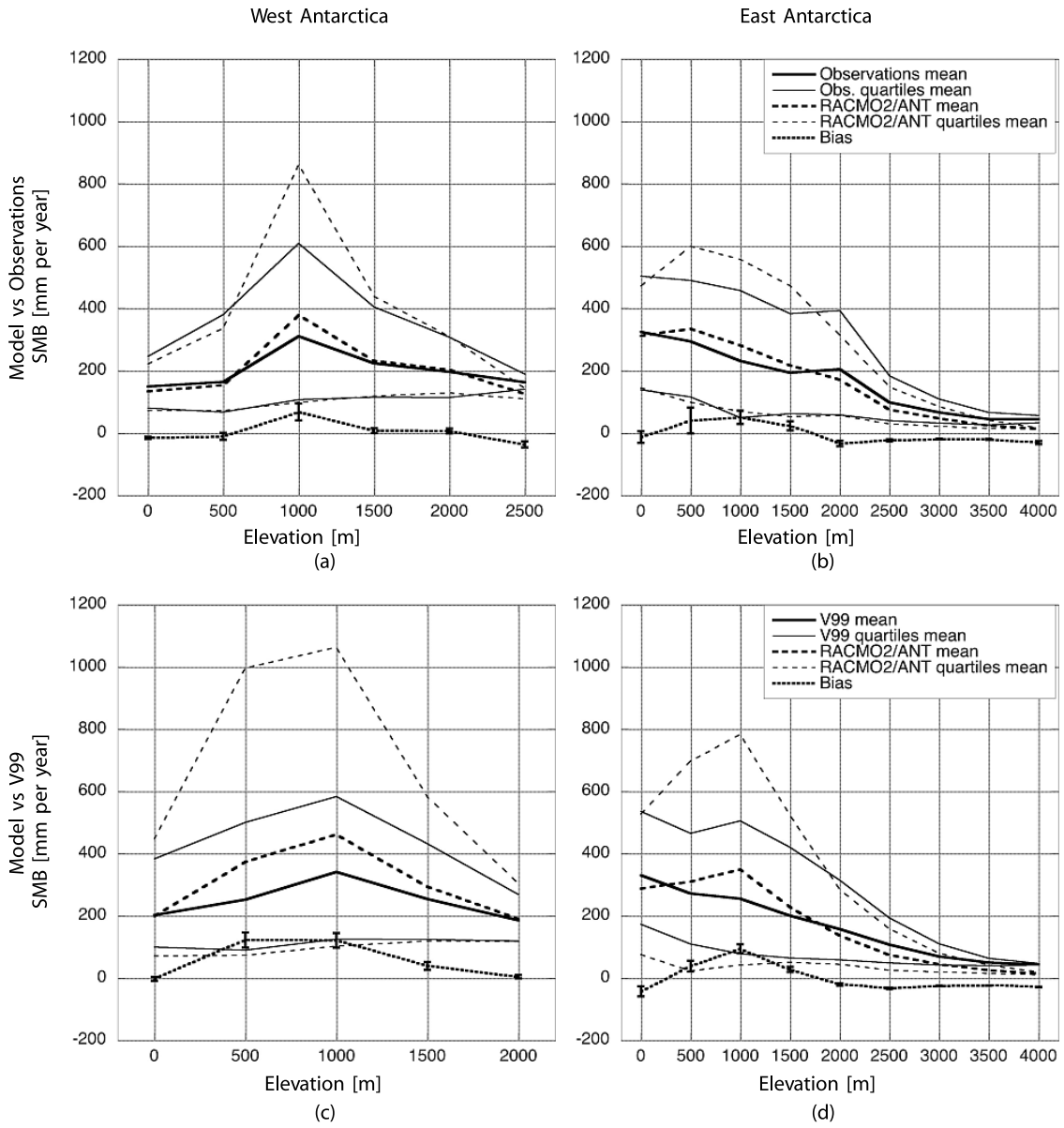

Figure 7. Comparison of model-simulated SMB with (a and b) observations and (c and d) V99 for West Antarctica (Figures 7a and 7c) and East Antarctica (Figures 7b and 7d), as a function of elevation. The thick lines display the bin average, and the thin lines display the bin average of the upper and lower quartiles. The bias is the mean difference between model-simulated SMB and V99/observations. The error bar is the statistical uncertainty on the bias.

covers elevations from sea level to 250 m asl. The limited data set inhibits a smaller bin size. Since the SMB data is not normally distributed and thus standard deviations are improper, the averages of the upper and lower quartile are shown instead. In this case the tail to a high SMB is often much longer than the tail to a low SMB. The error bar on the bias displays the uncertainty on the bias and not the standard deviation.

[39] The agreement between the model-simulated and observed SMB for West Antarctica (Figure 7a) is good. The biases are small, only around 1000 m height the bias is clearly positive. Also, the distribution of the SMB is simulated well, even though the upper quartile mean is overestimated around 1000 m height. Another sign of the quality of the model simulation is that the correlations inside bins are all very high, between 0.75 and 0.91.

[40] In East Antarctica (Figure 7b), RACMO2/ANT overestimates the SMB for high accumulation sites between 250 and 1750 m. On the plateau the distribution width is simulated well, but the mean SMB is 25 mm yr^{-1} too low for all plateau bins. Since the SMB gradually decreases uphill, relative deficiencies increase to more than 50% at 4000 m. The correlation inside bins is around 0.7 for all bins, except for 250 to 750 m asl, for which the correlation is 0.54. However, only 18 observations are available for this elevation bin, while the variability is large. New observa-

Table 2. Effect of Observation Handling[a]

Adjustment	N_{eff}	Correlation	Regression Slope
Default analysis[b]	1225	0.82	1.21 ± 0.06
No areas excluded	1281	0.69	1.7 ± 0.2
Fit to most nearby model grid point	1225	0.78	1.40 ± 0.09
Smoothed model output for dx_{max} = 193 km	1225	0.84	1.06 ± 0.04
Weight decreases quadratically	1225	0.82	1.20 ± 0.06
Weight scaling $\gamma = -0.5$	1373	0.82	1.21 ± 0.05
Weight scaling $\gamma = -1.0$	1110	0.82	1.21 ± 0.06
Outliers removed ($\|da\| <= 300$ mm)	1205	0.87	1.08 ± 0.01
Unequal measurement error		0.81	1.14 ± 0.04
Effect of elevation biases ($\|dh\| <= 250$ m)	1193	0.82	1.23 ± 0.06

[a]The results are derived using all observations over Antarctica except from the excluded areas, unless noted otherwise. The effective data amount N_{eff} is the sum of β_o over all included observations. The correlations and regression slopes are from the comparison between model and observations.
[b]Exclude areas, dx_{max} = 55 km, linear decreasing weight, $\gamma = -0.75$.

tions of SMB from the coastal zones of Antarctica are therefore urgently required.

[41] Figures 7c and 7d compare model-simulated SMB with V99. Figures 7c and 7d are based on many more data points. Striking differences with Figures 7a and 7b are visible. The model-simulated SMB and its spread are larger than V99 in the escarpment zones of both East and West Antarctica. Nevertheless, the correlation inside all bins is between 0.7 and 0.8. An exception is the lowest 250 m in East Antarctica, for which the correlation is only 0.41.

5. Discussion

5.1. Statistical Robustness of the Results

[42] Before the implications of the model results will be discussed, their statistical robustness will be considered. The statistical analysis consisted of a number of steps, which all could influence the final results (Table 2).

[43] First, observations from some parts of Antarctica (Antarctic Peninsula, Law Dome, coastal Marie Byrd Land) were excluded as discussed in section 3.1. Model-simulated SMB interpolated to the observation location, matches the observations less well for these regions, as can be concluded from the decrease in correlation coefficient when they are not omitted.

[44] Second, the model-simulated SMB is interpolated from model grid points to the observation locations, using equation (1). The default interpolation distance is 55 km, which implies that observations are nearly linearly interpolated between the 4 nearest grid points. If simply the model SMB of the nearest grid point is used, the correlation deteriorates. When model output is smoothed, the correlation improves. A maximum correlation is found for dx_{max} is 193 km. Simultaneously, the regression slope gradually decreases from 1.40 using the nearest grid point method to 1.06 for dx_{max} is 193 km. The decrease of the regression slope is a logical result of smoothing. From the fact that a certain amount of smoothing yields an improvement of correlation and the regression slope, we may conclude that the model-simulated SMB distribution has somewhat too pronounced gradients.

[45] Equation (1) uses a linear decrease of the relative weight for increasing distance. A test with a quadratical decrease of the relative weight leads to nearly equal results.

[46] Third, observations have been weighted in order to balance the unequal spatial distribution of measurements. However, the weight function is more or less arbitrary. Fortunately, tests with different values of γ in equation (3) show that this has no impact on the results.

[47] We conclude that these three steps of the data analysis procedure do not strongly influence the final results, except that some additional smoothing would improve the correlation between model-simulated and observed data.

[48] Additionally, the assumptions behind the statistics are validated. A properly determined regression line assumes a smooth distribution of the data, a requirement which is not fully satisfied as visible in Figure 6d. If outliers are removed, the slope of the regression decreases, because for about two thirds of the outliers the model-simulated SMB exceeds the observation. The result for a maximum accepted difference of 300 mm is given in Table 2 as an example. Another way to deal with nonhomogeneous data distribution is by using an additional weight that incorporates a linearly increasing error margin for the model simulated and observed SMB. Table 2 shows the results for the assumption that the error margin for a SMB of 200 mm is twice that of a SMB of 0 mm. In line with this particular example, the regression slope decreased for stronger weighting. Concluding, both inquiries give a decrease of the regression slope toward one, which affirms that the model-simulated distribution of the SMB is close to the observed one and that the correlation has not been strongly influenced by the data distribution.

[49] A final source of error could be elevation differences between the observation site and the representative grid box. The observed elevation may be inaccurate or it may not match model elevation in the case of small-scale topographic features. If such observations are removed the correlation slightly improves, but the regression slope remains unchanged. The impact on the results is thus small.

5.2. An Evaluation of Model Performance

[50] The detailed comparison with observations in section 4.2 and 4.4 revealed that RACMO2/ANT underestimates the SMB on the plateau of East Antarctica. The bias is between 20 and 44 mm yr^{-1}. Most contemporary numerical SMB estimates [*Bromwich et al.*, 2004; *Genthon and Krinner*, 2001; *Van Lipzig et al.*, 2002] show a similar underestimation of the SMB on the plateau. Diamond dust has been shown to contribute significantly to the SMB on the plateau [*Ekaykin et al.*, 2004]. Since diamond dust,

Table 3. Regression Quantities of Different Data Sets Compared to Observations[a]

Observations Compared With	Correlation	Regression Slope
Observations interpolated to grid points	0.971	0.945 ± 0.010
Vaughan et al. [1999]	0.928	0.94 ± 0.02
RACMO2/ANT	0.82	1.21 ± 0.06
Interpolated mean SMB for 500 m elevation bins	0.59	0.39 ± 0.02

[a]All observations are used, except from excluded areas (see text).

which essentially is a removal of boundary layer cloud ice, is not yet specifically parameterized in the model physics, the underestimated SMB is likely in part due to this neglected process.

[51] For the remainder of Antarctica, a direct comparison with observations shows a very reasonable agreement. The range of the SMB is simulated well, although slightly overestimated in some cases, and the correlation between the model-simulated and observed longitudinal variations is high. Moreover, model-simulated SMB is more accurate than would be expected from a direct comparison with V99.

[52] A quantitative assessment of model performance is listed in Table 3. First, observations of SMB are compared with the weighted mean of observations on grid points, using equation 5. This interpolation removes all patterns smaller than 55 km. The deviation of the correlation from one indicates the amount of such small-scale patterns in the observation data set. The value does not represent the average contribution of small-scale variability on the total spatial variability of the SMB of Antarctica, because in that case a high observation density for whole Antarctica is required.

[53] Second, the observations are compared to V99 data, choosing the nearest value in the original 10 km grid. It is no surprise that the compilation resembles the observations adequately. If V99 is compared to new observations that were not used in the compilation, the correlation is 0.75. The correlation of RACMO2/ANT to these new data is 0.82, similar as for the whole data set.

[54] Finally, the observations are compared with the observed mean of their elevation. This mean is linearly interpolated from the results as given in Figures 7a and 7b. The results shows that a simple SMB estimate based on elevation is still significantly correlated with the observations, but that a significant fraction of the variance explained is lost. Moreover, the spread of the SMB in Antarctica is severely underestimated, because the regression slope is far below one. We conclude that the model-simulated SMB distribution doubles the variance explained in the observations as compared to very simple parameterizations, and is also better capable of representing the absolute values.

5.3. Toward a Better Understanding of Antarctic SMB

[55] In this section, the calibration of model results to fit observations is discussed. The calibration aims at retrieving a SMB distribution that is as correct as possible. In contrast, an intelligent interpolation of the observations using RACMO2/ANT data as background field would have focused on regional correct distributions. The calibration performed here gives insight in the major remaining uncertainties of the contemporary spatial SMB of Antarctica.

[56] In section 4.4, the bias and slope of the regression line were derived for each elevation bin in East and West Antarctica. If the model results would have matched the observations perfectly, the bias would be zero and the regression slope one. An adjustment of the model results toward these perfect fits only improves the results if the correlation between observations and model in a bin is significant. Most elevation bins have a high and strongly significant correlation, which makes a correction feasible.

[57] The model-simulated SMB (SMB_g) is calibrated to $SMB_{g,c}$ with

$$SMB_{g,c} = \frac{SMB_g - \overline{SMB}_{mod}}{\max(0.9, s^{\zeta})} + \overline{SMB}_o, \tag{6}$$

in which $\overline{SMB}_{mod}$ and $\overline{SMB}_o$ are the mean model-simulated and observed SMB for the elevation of the model grid point, respectively. The regression slope s to the power ζ scales the model-simulated SMB variability along elevation bands to observed variability, but only if the variability is larger than the observed variability. If this threshold is not applied, nonexisting variability might have been created. The values of $\overline{SMB}_{mod}$, $\overline{SMB}_o$ and s are linearly interpolated for each grid point from the binned results. Optimal results are found for $\zeta = 0.5$ and a threshold value of 0.9.

[58] Figure 8a shows the calibrated spatial SMB. The first main difference with the original model field is the 20–30 mm yr^{-1} wetter plateau of East Antarctica. Second, the accumulation in the coastal and escarpment zone between 500 and 1500 meter elevation is on average reduced with 15%. Note that the correction that is applied for the Antarctic Peninsula uses correction data from West Antarctica, so model results in this area must be interpreted with care. Furthermore, note that this correction is a calibration and not an interpolation of observations using model results as background, so locally the calibration might diverge model results from observations. The overall correlation with the observations increases slightly to 0.83 and the regression slope becomes 1.00.

[59] We also show the statistical uncertainty of the calibrated SMB in Figure 8b. This uncertainty is determined by repeating the calibration procedure 10.000 times using a randomly chosen one third of the observations. The resulting standard deviation is a measure of the uncertainty of the calibrated SMB distribution owing to the calibration procedure. For all locations the statistical uncertainty is one order of magnitude smaller than the SMB.

[60] Subsequently, Figure 9a shows the differences of the calibrated SMB with the observations. Although the calibration procedure did not focus on individual observations, overall the deviations have decreased (Figure 6c). These

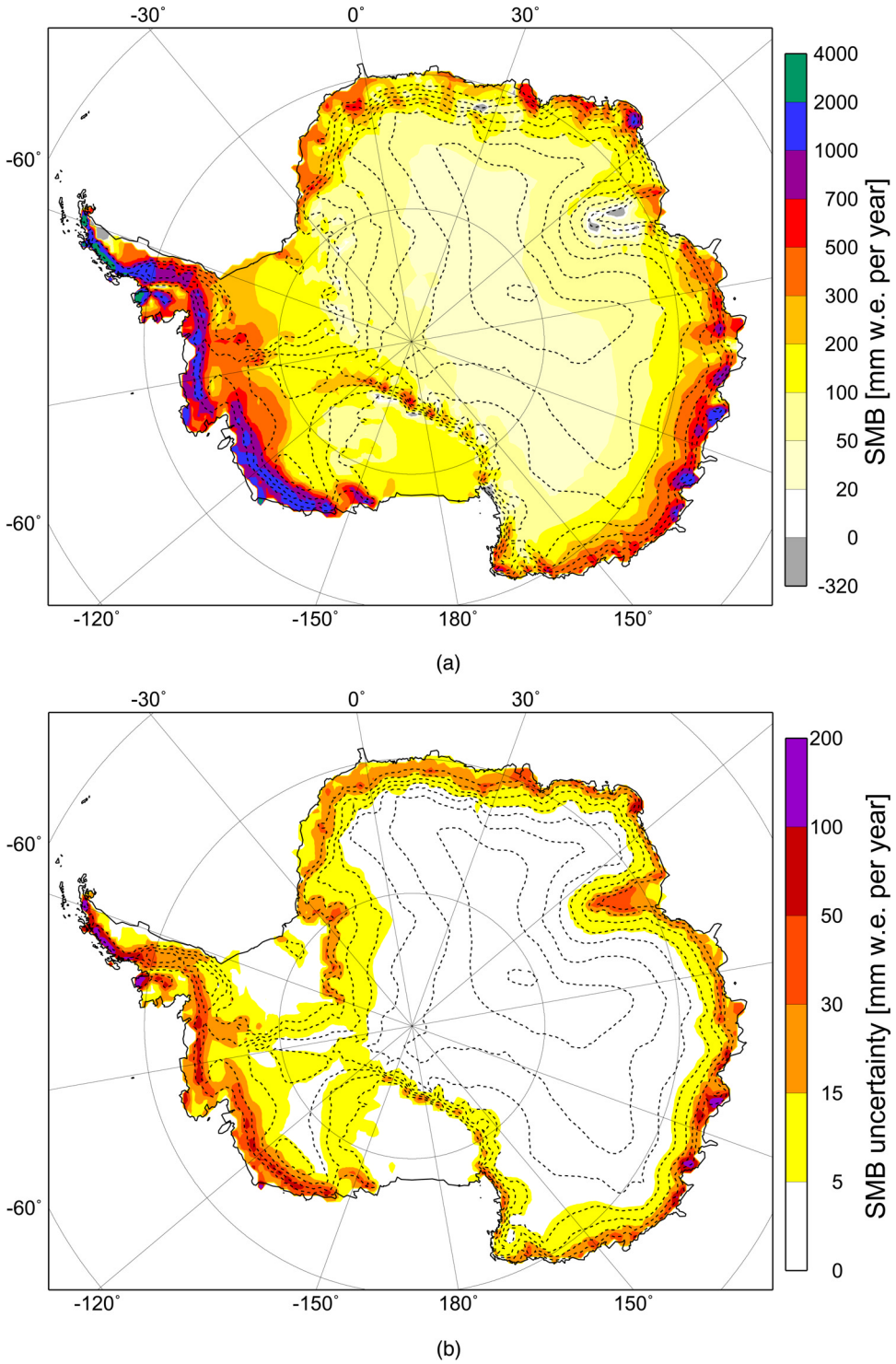

Figure 8. (a) Calibrated model SMB and (b) statistical uncertainty due to calibration procedure. Only model land points are shown. The SMB of the Antarctic Peninsula is calibrated using the data from West Antarctica.

improvements are clear for the interior of East Antarctica. Elsewhere, improvements are less traceable because of the scatter between model data and observations. Noteworthy is that within one transect the calibrated SMB is often strongly correlated to observations. Examples are the transects at 20° and 40° West and ~72° South.

[61] The calibrated SMB is compared to V99 in Figure 9b. For the most of Antarctica, the differences are closely connected with those in Figure 9a. Exceptions are the much higher model-simulated SMB in the coastal regions which are east of Law Dome in East Antarctica and the Amundsen and Bellingshausen Sea coast of West Antarctica. These differ-

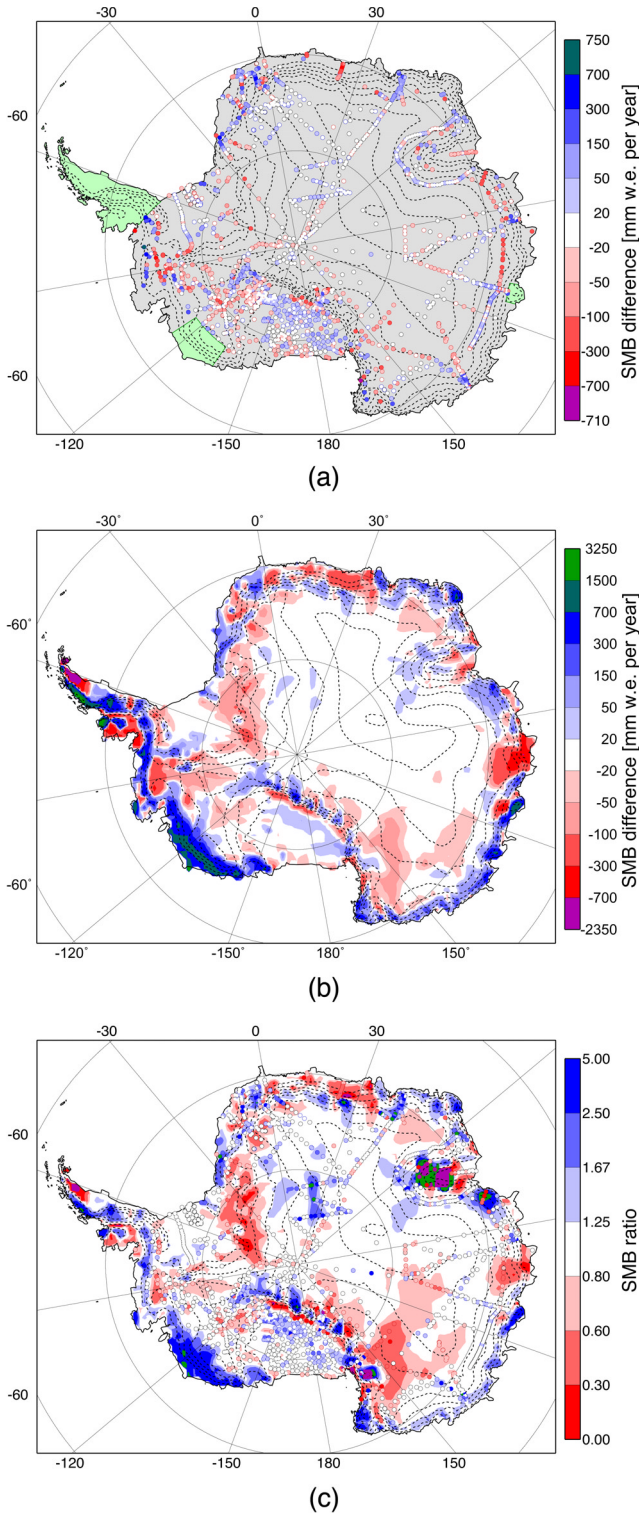

Figure 9. (a) Differences between calibrated model SMB and the observations that were used for the calibration. (b) Differences between calibrated model SMB and V99. (c) Continuous map showing the ratio between the calibrated model results and V99. The overlaid circles are the ratio between the calibrated model results and observations. Positive values indicate that the calibrated SMB is larger than the observations or V99.

ences are also much larger than the statistical uncertainty of the calibrated SMB, and exceed the range of deviations that is found between the calibrated model results and the observations.

[62] In Figure 9c the relative differences of the model with the compilation of V99 and the biases to the observations are shown. As indicated earlier, since V99 is a proper interpolation of almost all observations used in this manuscript, there is a general correspondence between the two. The biases are all within a reasonable limit. Consequently, significant deviations of the calibrated SMB fields with the compilation of V99 in areas poorly covered by observations, visible in the above listed regions, can unlikely be blamed on poor model performance. Therefore the SMB of these regions has likely been severely underestimated until now.

[63] Next, the model-simulated and calibrated SMB are averaged over the grounded ice sheet (GIS). RACMO2/ANT simulates an integrated SMB of 169 mm yr^{-1} for 1980 to 2004, the calibrated average SMB is 171 ± 3 mm yr^{-1}. This estimate is about 15% higher than the estimate of V99 (149 mm yr^{-1}). The calibrated SMB equals a total mass input to Antarctica of $2.08 \pm 0.03 \cdot 10^{15}$ kg yr^{-1} for the GIS and $2.52 \pm 0.03 \cdot 10^{15}$ kg yr^{-1} for the whole of Antarctica including ice shelves. These values are higher than all estimates listed by *IPCC* [2001, p. 651], but they are comparable with the recent model estimate from *Bromwich et al.* [2004] (Table 4). The increase of the SMB compared to the IPCC estimate represents an additional storage of water on Antarctica of 0.6 mm global sea level yr^{-1}. Since model results are calibrated with observations of which most cover an older time period, the likelihood is small that increased precipitation in the last two decades of the 20th century is the source for this difference.

[64] The largest uncertainties about the contemporary spatial SMB distribution in Antarctica lay in the coastal and escarpment regions. The sharp accumulation gradients and the large-scale longitudinal variations related to the upper air circulation [*Van Lipzig et al.*, 2002], combined with few observations, cause these uncertainties. Although these regions make up only a small fraction of the Antarctic continent, their impact on the integrated SMB is substantial because of the large average accumulation rates. If indeed the SMB of these regions is larger than previously thought, the annual mass input in the grounded ice sheet of Antarctica is larger than recent estimates have suggested. The only method to validate or disprove these results is to perform more SMB measurements in coastal areas of Antarctica.

6. Conclusions

[65] We made a detailed comparison of model-simulated and observed SMB in Antarctica, and calibrated the model-simulated SMB distribution to construct a best estimate of contemporary Antarctic SMB.

[66] The model results used here are from a regional atmospheric climate model (RACMO2/ANT) for the time period 1980 to 2004, using ERA-40 fields as lateral forcing. The model results of the period 1958–1979 are not used because of the poor quality of ERA-40 in the Southern Hemisphere before 1980 [*Bromwich and Fogt*, 2004].

Table 4. Estimated SMB, Integrated Over the Grounded Antarctic Ice Sheet or Including Ice Shelves and Compared to Recent Other Estimates as Listed by *IPCC* [2001]

Source	Remarks	GIS, 10^{12} kg yr^{-1}	All Ice Sheets, 10^{12} kg yr^{-1}
Turner et al. [1999]	atmospheric moisture budget analysis from ECMWF reanalysis, 1979 to 1993		2106
V99		1811	2288
Huybrechts et al. [2000]	updated accumulation map	1924	2344
Giovinetto and Zwally [2000]	updated map on 50 km grid	1883	2326
IPCC [2001, p. 651]	mean and standard deviation	1843 ± 76	2246 ± 86
Van Lipzig et al. [2002]	precipitation minus evaporation using RACMO1/ANT	1890 ± 90	
Bromwich et al. [2004]	precipitation minus evaporation using regional atmospheric model MM5		2572 ± 221
This study, 1980–2004		2076 ± 29	2521 ± 33

[67] We used all available SMB observations for the comparison. Observations were only discarded if clearly erroneous. Before the comparison, the individual weight of clustered observations was reduced, otherwise these areas would be overrepresented. Furthermore, the Law Dome area and the Antarctic Peninsula are left out of the comparison, because of small-scale topography that inhibit a meaningful quantitative comparison on model resolution (55 km). Model results for these areas have been discussed separately.

[68] Comparing model-simulated SMB with the compilation of *Vaughan et al.* [1999], a correlation of 0.79 and a regression slope of 1.7 is found. When model-simulated SMB is directly compared to observations, a correlation of 0.82 and a regression slope of 1.21 is found. The model-simulated SMB closely matches the observations and V99 in data covered regions, but does not agree with V99 in data-sparse regions. We binned the observations in 500 m elevation intervals for East and West Antarctica and compared these to model SMB in each bin separately. The correlation remains high (0.66 to 0.91) and the mean and distribution of the SMB compares well for most bins, although a systematic underestimation is found for the high plateau of East Antarctica. These results support the robustness of the model-simulated SMB and offers the possibility to calibrate model-simulated SMB without losing reliability.

[69] The main difference between calibrated model SMB and the compilation of V99 is a higher model SMB in the coastal zones of (eastern) East Antarctica and West Antarctica, without exception areas with few observations. Along the coast of Marie Byrd Land the differences reach 1 m w.e. yr^{-1}. These higher values result in a 15% higher estimate (171 ± 3 mm yr^{-1}) of the SMB integrated over the grounded ice sheet compared to V99. Despite the apparent small statistical uncertainty which is based on the calibration procedure only, this new estimate of Antarctic SMB is as reliable as the reliability that is credited to atmospheric models. Support or falsification of this result can only be found in new SMB observations from poorly covered high accumulation regions in coastal Antarctica.

[70] **Acknowledgments.** We would first like to thank David Vaughan for providing his SMB observation database and the data of his SMB compilation. We also would thank Massimo Frezzotti, Susan Kaspari, Hans Oerter and Roderik van der Wal for providing recent SMB observations. We are grateful to Elisabeth Isaksson, Lynn Lay, Nicole van Lipzig, Andrew Monaghan and Rob Mulvaney for their valuable help on various parts of this project.

References

Andreas, E. L. (1987), A theory for the scalar roughness and the scalar transfer coefficients over snow and sea ice, *Boundary Layer Meteorol.*, *38*, 159–184.

Box, J. E., D. H. Bromwich, and L.-S. Bai (2004), Greenland ice sheet surface mass balance 1999–2000: Application of Polar MM5 mesoscale model and in situ data, *J. Geophys. Res.*, *109*, D16105, doi:10.1029/2003JD004451.

Box, J. E., D. H. Bromwich, B. A. Veenhuis, L.-S. Bai, J. C. Stroeve, J. C. Rogers, K. Steffen, T. Haran, and S.-H. Wang (2006), Greenland ice sheet surface mass balance variability (1988–2004) from calibrated Polar MM5 output, *J. Clim.*, in press.

Bromwich, D., and R. L. Fogt (2004), Strong trends in the skill of the ERA-40 and NCEP-NCAR reanalyses in the high and midlatitudes of the Southern Hemisphere, 1958–2001, *J. Clim.*, *17*, 4603–4619.

Bromwich, D. H., Z. Guo, L. Bai, and Q.-S. Chen (2004), Modeled Antarctic precipitation. Part I: Spatial and temporal variability, *J. Clim.*, *17*, 427–447.

Bull, C. (1971), Snow accumulation in Antarctica, in *Research in the Antarctic*, vol. 2, pp. 367–421, Am. Assoc. for the Adv. of Sci., Washington, D. C.

Davis, C., Y. Li, J. R. McConnell, M. M. Frey, and E. Hanna (2005), Snowfall-driven growth in East Antarctic Ice Sheet mitigates recent sea-level rise, *Science*, *308*, 1898–1901, doi:10.1126/science.1110662.

Dethloff, K., M. Schwager, J. H. C. S. Kiilsholm, A. Rinke, W. Dorn, F. Jung-Rothenhäusler, H. Fischer, S. Kipfstuhl, and H. Miller (2002), Recent Greenland accumulation estimated from regional climate model simulations and ice core analysis, *J. Clim.*, *15*(19), 2821–2832.

Ekaykin, A. A., V. Y. Lipenkov, I. N. Kuzmina, J. R. Petit, V. Masson-Delmotte, and S. J. Johnsen (2004), The changes in isotope composition and accumulation of snow at Vostok station, East Antarctica, over the past 200 years, *Ann. Glaciol.*, *39*, 569–575.

Frezzotti, M., et al. (2004), New estimations of precipitation and surface sublimation in East Antarctica from snow accumulation measurements, *Clim. Dyn.*, *23*(7–8), 803–813.

Genthon, C., and G. Krinner (2001), Antarctic surface mass balance and systematic biases in general circulation models, *J. Geophys. Res.*, *106*(D18), 20,653–20,664.

Giovinetto, M. B., and H. J. Zwally (2000), Spatial distribution of net surface accumulation on the Antarctic ice sheet, *Ann. Glaciol.*, *31*, 171–178.

Hofstede, C. M., et al. (2004), Firn accumulation records for the past 1000 years on the basis of dielectric profiling of six cores from Dronning Maud Land, Antarctica, *J. Glaciol.*, *50*(169), 279–291.

Huybrechts, P., D. Steinhage, F. Wilhelms, and J. Bamber (2000), Balance velocities and measured properties of the Antarctic ice sheet from a new compilation of gridded data for modelling, *Ann. Glaciol.*, *30*, 52–60.

Intergovernmental Panel on Climate Change (IPCC) (2001), *Climate Change 2001: The Scientific Basis. Contribution of Working Group 1 to the Third Assessment Report of the Intergovernmental Panel on Climate Change*, Cambridge Univ. Press, New York.

Kärlof, L., et al. (2000), A 1500 year record of accumulation at Amundsenisen western Dronning Maud Land, Antarctica, derived from electrical and radioactive measurements on a 120 m ice core, *J. Geophys. Res.*, *105*, 12,471–12,483.

Kaspari, S., P. A. Mayewski, D. A. Dixon, V. B. Spikes, S. B. Sneed, M. J. Handley, and G. S. Hamilton (2004), Climate variability in West Antarctica derived from annual accumulation rate records from ITASE firn/ice cores, *Ann. Glaciol.*, *39*, 585–594.

Lenderink, G., B. van den Hurk, van E. Meijgaard, A. van Ulden, and H. Cuijpers (2003), Simulation of present-day climate in RACMO2: First results and model developments, *Tech. Rep. TR-252*, R. Dutch Meteorol. Inst., De Bilt, Netherlands.

Liu, H., K. Jezek, B. Li, and Z. Zhao (2001), Radarsat Antarctic Mapping Project Digital Elevation Model Version 2, http://nsidc.org/data/nsidc-0082.html, Natl. Snow and Ice Data Cent., Boulder, Colo.

Magand, O., M. Frezzotti, M. Pourchet, B. Stenni, L. Genoni, and M. Fily (2004), Climate variability along latitudinal and longitudinal transects in East Antarctica, *Ann. Glaciol.*, *39*, 351–358.

Oerter, H., W. Graf, F. Wilhelms, A. Minikin, and H. Miller (1999), Accumulation studies on Amundsenisen, Dronning Maud Land, by means of tritium, dielectric profiling and stable-isotope measurements: First results from the 1995–96 and 1996–97 field seasons, *Ann. Glaciol.*, *29*, 1–9.

Oerter, H., F. Wilhelms, F. Jung-Rothenhäusler, F. Göktas, H. Miller, W. Graf, and S. Sommer (2000), Accumulation rates in Dronning Maud Land, Antarctica, as revealed by dielectric-profiling measurements of shallow firn cores, *Ann. Glaciol.*, *30*, 27–34.

Pirrit, J., and G. A. Doumani (1961), Glaciology, Byrd Station and Mary Byrd Land Traverse, 1959–1960, *Tech. Rep. Proj. 968 Rep. 2*, Ohio State Univ., Columbus.

Reijmer, C. H., E. van Meijgaard, and M. R. van den Broeke (2004a), Evaluation of temperature and wind over Antarctica in a regional atmospheric climate model using 1 year of automatic weather station data and upper air observations, *J. Geophys. Res.*, D04103, doi:10.1029/2004JD005234.

Reijmer, C. H., E. van Meijgaard, and M. R. van den Broeke (2004b), Numerical studies with a regional atmospheric climate model based on changes in the roughness length for momentum and heat over Antarctica, *Boundary Layer Meteorol.*, *111*, 313–337.

Rogers, R. R., and M. K. Yau (1989), *A Short Course in Cloud Physics*, *Int. Ser. Nat. Philos.*, vol. 113, 3rd ed., Elsevier, New York.

Smith, B. T., T. D. van Ommen, and V. I. Morgan (2002), Distribution of oxygen isotope ratios and snow accumulation rates in Wilhelm II Land, East Antarctica, *Ann. Glaciol.*, *35*, 107–110.

Sterl, A. (2004), On the (in-)homogeneity of reanalysis products, *J. Clim.*, *17*, 3866–3873.

Thomas, R., et al. (2004), Accelerated sea-level rise from West Antarctica, *Science*, *306*, 255–258.

Turner, J., W. M. Connolley, S. Leonard, G. J. Marshall, and D. G. Vaughan (1999), Spatial and temporal variability of net snow accumulation over the Antarctic from ECMWF re-analysis project data, *Int. J. Climatol.*, *19*, 697–724.

Turner, J., T. A. Lachlan-Cope, G. J. Marshall, E. M. Morris, R. Mulvaney, and W. Winter (2002), Spatial variability of Antarctic Peninsula net surface mass balance, *J. Geophys. Res.*, *107*(D13), 4173, doi:10.1029/2001JD000755.

Undén, P., et al. (2002), The high resolution limited area model, Hirlam-5 scientific documentation, report, 144 pp., Swed. Meteorol. and Hydrol. Inst., Norrköping.

Van de Berg, W. J., M. R. van den Broeke, C. H. Reijmer, and E. van Meijgaard (2006), Characteristics of the Antarctic surface mass balance (1958–2002) using a regional atmospheric climate model, *Ann. Glaciol.*, in press.

Van den Broeke, M. R., J.-G. Winther, E. Isaksson, J. F. Pinglot, L. Karlöf, T. Eiken, and L. Conrads (1999), Climate variables along a traverse line in Dronning Maud Land, East Antarctica, *J. Glaciol.*, *45*(150), 295–302.

Van den Hurk, B., and P. Viterbo (2003), The Torne-Kalix PILPS 2e experiment as a test bed for modifications to the ECMWF land surface scheme, *Global Planet. Change*, *38*, 165–173.

Van Lipzig, N. P. M., E. van Meijgaard, and J. Oerlemans (2002), The spatial and temporal variability of the surface mass balance of Antarctica: Results from a regional atmospheric climate model, *Int. J. Climatol.*, *22*, 1197–1217.

Van Lipzig, N. P. M., J. C. King, T. A. Lachlan-Cope, and M. R. van der Broeke (2004), Precipitation, sublimation, and snow drift in the Antarctic Peninsula region from a regional atmospheric model, *J. Geophys. Res.*, *109*, D24106, doi:10.1029/2004JD004701.

van Ommen, T. D., V. Morgan, and M. A. J. Curran (2004), Deglacial and Holocene changes in accumulation at Law Dome, *Ann. Glaciol.*, *39*, 359–365.

Vaughan, D. G., J. L. Bamber, M. Giovinetto, and A. P. R. Cooper (1999), Reassessment of net surface mass balance in Antarctica, *J. Clim.*, *12*, 933–946.

White, P. W. (2001), IFS documentation (CY23R4), part IV, Physical processes, technical report, 101 pp., Eur. Cent. for Medium-Range Weather Forecasts, Reading, U. K.

Zwally, H., and M. Giovinetto (1995), Accumulation in Antarctica and Greenland derived from passive-microwave data: A comparison with contoured compilations, *Ann. Glaciol.*, *21*, 123–130.

C. H. Reijmer, W. J. van de Berg, and M. R. van den Broeke, IMAU, Universiteit Utrecht, Princetonplein 5, NL-3584 CC Utrecht, Netherlands. (w.j.vandeberg@phys.uu.nl)

E. van Meijgaard, KNMI, Wilhelminalaan 10, NL-3732 GK De Bilt, Netherlands.